Selected Paper

Electroabsorption and Electrophotoluminescence Spectra of Porphyrin Supramolecules in a Polymer Film

Takakazu Nakabayashi,[1] Takefumi Yotsutsuji,[2] Kazuya Ogawa,*[2,3] Yoshiaki Kobuke,[2,4] and Nobuhiro Ohta*[1]

[1]Research Institute for Electronic Science (RIES), Hokkaido University, Sapporo 001-0020

[2]Graduate School of Materials Science, Nara Institute of Science and Technology, 8916-5 Takayama, Ikoma 630-0101

[3]Interdisciplinary Graduate School of Medicine and Engineering, University of Yamanashi, 4-3-11 Takeda, Kofu 400-8511

[4]Institute of Advanced Energy, Kyoto University, Gokasho, Uji, Kyoto 611-0011

Received October 5, 2009; E-mail: nohta@es.hokudai.ac.jp

Electroabsorption and electrophotoluminescence spectra of supramolecular porphyrin dimers in a solid film of poly(methyl methacrylate), PMMA, have been examined. The electroabsorption spectra in the Soret band region are fitted by the deconvolution of the corresponding absorption spectrum into four components, indicating that electroabsorption measurements are useful to identify bands that are hard to distinguish in absorption spectra. The values of the changes in molecular polarizability and dipole moment following photoexcitation are evaluated at each absorption band.

Supramolecular systems with porphyrins have been extensively studied as building blocks of artificial photosynthetic systems and as photonic and electronic devices. A variety of porphyrin-based supramolecules have been reported either by covalent or non-covalent approaches.[1–8] Non-covalent approaches have the merit of allowing facile construction of multi-porphyrin arrays and porphyrin-based donor/acceptor complexes. The strong interaction between two porphyrins can also be performed by self-organization via ligand-to-metal coordination.[1–3]

In the present study, we have measured electric field effects on absorption and photoluminescence spectra of the dimers of *meso*-imidazolyl-substituted zinc porphyrins. Chemical structures of the porphyrin dimers used in the present study are shown in Figure 1. A complementary coordination of imidazolyl to zinc affords the dimer formation with a slipped cofacial arrangement, resulting in a close proximity of the two porphyrin surfaces.[1–3] These dimers exhibit a large splitting of the Soret absorption band, indicating strong exciton coupling between the two porphyrins. These dimers therefore are regarded as a good mimic of the special pair in photosynthetic reaction centers. Such a slipped cofacial dimer with self-coordination can also be developed to obtain a giant porphyrin array containing up to 800 porphyrin units even in a dilute $CHCl_3$ solution.[9] Multi-porphyrin systems based on the slipped cofacial dimer exhibit excellent optical properties such as a large third-order optical nonlinearity[10] and a strong two-photon absorption.[11] Detailed knowledge of the electronic structures of supramolecular porphyrin systems is essential for optimizing optical properties for specific applications.

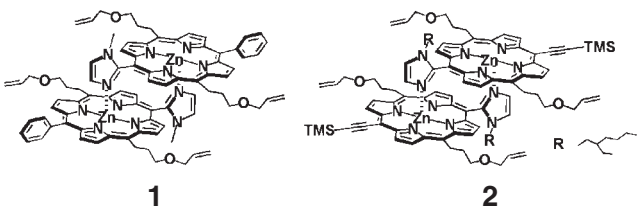

Figure 1. Structures of porphyrin supramolecules used in the present study.

External electric field effects on optical spectra have been extensively used in molecular spectroscopy to examine electronic structures in excited states.[12–21] The electroabsorption and electrophotoluminescence spectra (plots of the electric-field-induced change in absorption intensity and photoluminescence, PL, intensity, respectively, as a function of wavelength or wavenumber) provide information on the differences in electric dipole moment ($\Delta\boldsymbol{\mu}$) and molecular polarizability ($\Delta\boldsymbol{\alpha}$) between the ground and excited states.[12–21] Measurements of these spectra are also very useful to clarify the mechanism of photoexcitation dynamics.[14] Here, we have estimated the values of $\Delta\boldsymbol{\mu}$ and $\Delta\boldsymbol{\alpha}$ for the absorption and PL (fluorescence) bands of the dimers, and identified several absorption bands that are difficult to distinguish in the absorption spectra. Hereafter, electroabsorption and electrophotoluminescence spectra are abbreviated as E-A and E-PL spectra, respectively, and applied external electric field is denoted by $\boldsymbol{F}$.

Theoretical

A shift of energy level induced by $\boldsymbol{F}$ is well known as the Stark shift, and the magnitude of this effect depends on the electric dipole moment ($\boldsymbol{\mu}$) and the molecular polarizability ($\boldsymbol{\alpha}$) of the state concerned. When the magnitude of $\boldsymbol{\mu}$ or $\boldsymbol{\alpha}$ in the excited electronic state is different from that in the ground state, the absorption spectra as well as the emission spectra are

Published on the web December 18, 2009; doi:10.1246/bcsj.20090264

shifted since the magnitudes of the level shift in both states are different from each other. According to the theory of electric field effects on optical spectra,[12,16] the field-induced change in absorption intensity of an isotropically-distributed sample in rigid matrices such as PMMA at wavenumber ν, i.e., $\Delta A(\nu)$, is given by a sum of the zeroth, first, and second derivatives of the absorption $A(\nu)$ as follows:

$$\Delta A(\nu) = (f\boldsymbol{F})^2\left[A'A(\nu) + B'\nu\frac{\mathrm{d}\{A(\nu)/\nu\}}{\mathrm{d}\nu} + C'\nu\frac{\mathrm{d}^2\{A(\nu)/\nu\}}{\mathrm{d}\nu^2}\right] \quad (1)$$

where f is the internal field factor. The coefficient A' depends on the transition polarizability and transition hyperpolarizability, and B' and C' are approximately given by the following forms:

$$B' = \frac{\Delta\bar{\alpha}/2 + (\Delta\alpha_{\mathrm{m}} - \Delta\bar{\alpha})(3\cos^2\chi - 1)/10}{hc} \quad (2)$$

$$C' = |\Delta\boldsymbol{\mu}|^2\frac{[5 + (3\cos^2\xi - 1)(3\cos^2\chi - 1)]}{30h^2c^2} \quad (3)$$

where $\Delta\bar{\alpha}$ denotes the trace of $\Delta\boldsymbol{\alpha}$, i.e., $\Delta\bar{\alpha} = (1/3)\mathrm{Tr}(\Delta\boldsymbol{\alpha})$; $\Delta\alpha_{\mathrm{m}}$ is the diagonal component of $\Delta\boldsymbol{\alpha}$ with respect to the direction of the transition dipole moment; χ is the angle between the direction of $\boldsymbol{F}$ and the electric vector of the light; and ξ is the angle between the direction of $\Delta\boldsymbol{\mu}$ and the transition dipole moment. At the magic angle condition, i.e., $\chi = 54.7°$, the coefficient B' and C' are reduced, respectively, as

$$B' = \frac{\Delta\bar{\alpha}}{2hc} \quad (4)$$

$$C' = \frac{|\Delta\boldsymbol{\mu}|^2}{6h^2c^2} \quad (5)$$

From eqs 4 and 5, the values of $\Delta\bar{\alpha}$ and $|\Delta\boldsymbol{\mu}|$ can be obtained from the first and second derivative components of the E-A spectrum, respectively.

The E-PL spectrum ($\Delta I_{\mathrm{F}}(\nu)$) is also given by the following equation:[14]

$$\Delta I_{\mathrm{F}}(\nu) = (f\boldsymbol{F})^2\left[A''I_{\mathrm{F}}(\nu) + B''\nu^3\frac{\mathrm{d}\{I_{\mathrm{F}}(\nu)/\nu^3\}}{\mathrm{d}\nu} + C''\nu^3\frac{\mathrm{d}^2\{I_{\mathrm{F}}(\nu)/\nu^3\}}{\mathrm{d}\nu^2}\right] \quad (6)$$

The first and second derivative components arise from $\Delta\boldsymbol{\alpha}$ and $\Delta\boldsymbol{\mu}$, respectively. The zeroth derivative component, which corresponds to the field-induced change in emission quantum yield, arises from the field-induced change in radiative decay rate and/or in non-radiative decay rate at the emission state. Then, the electric field effects on photoexcitation dynamics can be evaluated from the zeroth derivative component of the E-PL spectrum.

Results and Discussion

The E-A spectra of **1** and **2** in a PMMA film are shown in Figure 2, together with the corresponding absorption spectra. The E-A spectra were measured with a field strength of $0.7\,\mathrm{MV\,cm^{-1}}$ at the magic angle condition for $\chi = 54.7°$. As shown in the figure, the Soret absorption band in the region of 400–500 nm splits by ca. 1300 and $1100\,\mathrm{cm^{-1}}$ for **1** and **2**, respectively, indicating that the slipped cofacial arrangement remains unchanged in a PMMA polymer film. The π-conjugation of porphyrin in **2** is expanded by introducing a TMS–ethynyl group, inducing a red-shift not only of the Soret band but also of the Q band in the region of 550–650 nm. The shape of the E-A spectrum is remarkably different from that of the absorption spectrum; each absorption band shows characteristic field dependence. The shapes of the E-A spectra were not affected by the change of the field strength up to $1.0\,\mathrm{MV\,cm^{-1}}$.

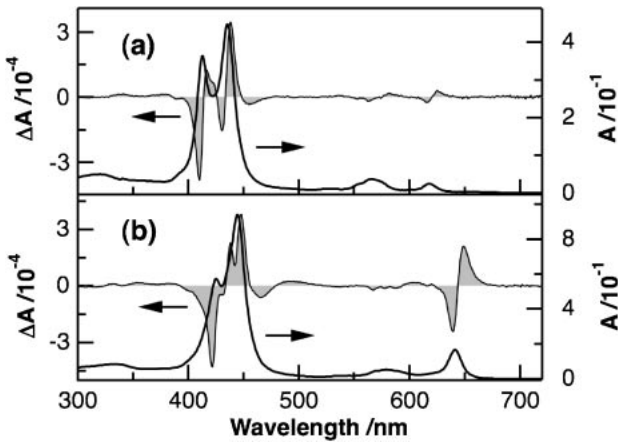

Figure 2. Absorption spectra (solid line) and electroabsorption spectra (shaded line) of **1** (a) and **2** (b) in a PMMA film. Applied field strength was $0.7\,\mathrm{MV\,cm^{-1}}$.

As mentioned above, the E-A spectra are given by a sum of the zeroth, first, and second derivative spectra of the absorption spectrum. From the coefficients of the first and second derivative components, the values of $\Delta\bar{\alpha}$ and $|\Delta\boldsymbol{\mu}|$ following photoexcitation can be obtained. To perform the detailed analysis of the E-A spectra in the Soret band region, we first tried to reproduce the E-A spectra with a linear combination of the zeroth, first, and second derivatives of the corresponding absorption spectrum according to eq 1. However, a disagreement between the simulated and observed spectra was obtained for both E-A spectra, suggesting that different absorption bands give different $\Delta\bar{\alpha}$ and $|\Delta\boldsymbol{\mu}|$ values from each other. We have therefore deconvoluted the absorption spectra in the Soret band region into four components (two large (L_1 and L_3) and two small (L_2 and L_4) bands as shown in Figures 3a and 3c) and simulated the E-A spectra with the derivatives of each decomposed band. The fitted results for the absorption and E-A spectra are shown in Figure 3. The E-A spectra of **1** and **2** in the Soret band region can be well fitted by the decomposition of the corresponding absorption spectrum into the four components. The decomposition into two bands is insufficient to fit the E-A spectra (Figures 3b and 3d). Especially, the negative E-A intensity in the region of 21000–$22000\,\mathrm{cm^{-1}}$ cannot be reproduced by considering only two components.

All the decomposed absorption bands are assumed to be Lorentzian. In Figures 3a and 3c, two small bands (L_2 and L_4) that are difficult to distinguish in the absorption spectra are identified from the E-A spectra, suggesting that at least four absorption bands (L_1–L_4 in Figure 3) are included in the absorption spectra of **1** and **2** in a PMMA polymer film. As mentioned above, the Soret band splits due to the interaction between porphyrins, and the magnitude and the direction of the

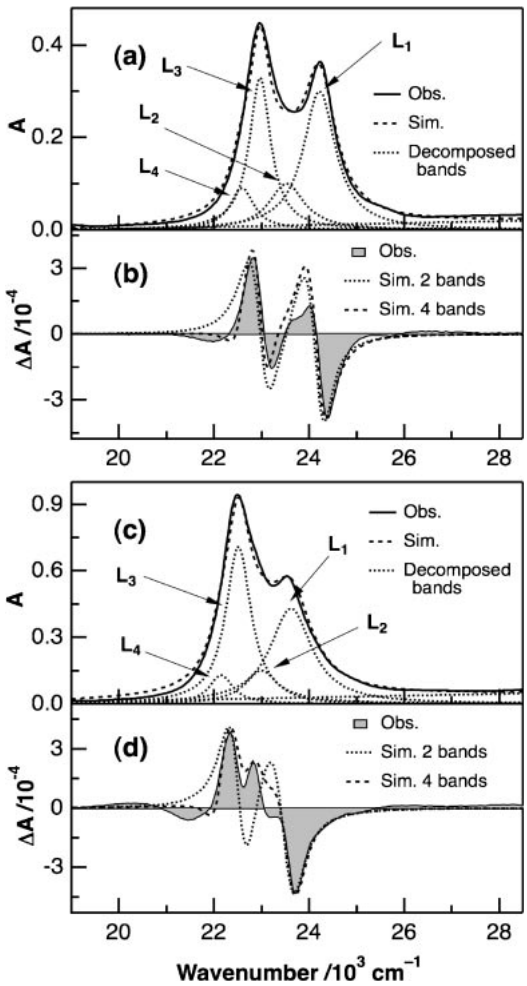

Figure 3. (a, c) Absorption spectra (solid line) of **1** (a) and **2** (c) in a PMMA film in the Soret band region together with the simulated ones (thick-dotted line). Decomposed bands (L_1–L_4) and background lines are also shown by thin-dotted lines. (b, d) Electroabsorption spectra (shaded line) of **1** (b) and **2** (d). Thin-dotted and thick-dotted lines are the spectra simulated with the decomposition of the absorption spectrum into two (L_1 and L_3) and four bands, respectively. Applied field strength was 0.7 MV cm^{-1}.

shift depend on the distance and the relative orientation of porphyrins.[1–3] It is thought that the degenerate Soret transitions in the monomeric unit split due to the head-to-tail or face-to-face orientations of the transition dipoles in the slipped cofacial arrangement, respectively. However, if the orientation of two porphyrin rings is slightly deviated from the right place due to interactions with PMMA, all of the four exciton bands become optically allowed. It may thus be possible that the observed four absorption bands are assigned to the four exciton bands of the porphyrin dimer, although the face-to-face interaction seems to be dominant because the two small bands (L_2 and L_4) appear in a lower-wavenumber region of the nearby strong band. It may be also possible to consider that the two small bands identified by the E-A spectra arise from different supramolecular conformers: one major and some interaction modes of the porphyrin dimer exist in a PMMA polymer film. In general, two or more species are often observed in a PMMA film arising from different interaction modes between PMMA and dissolved molecules.[17] The generation of other species by an applied field can be ruled out because the present field strength was sufficiently low only to exhibit a small shift in energy level.[13–16]

Table 1. The Values of $\Delta\bar{\alpha}$ and $|\Delta\boldsymbol{\mu}|$ for Photoexcitation into Each of the Soret Bands and the Q Bands of **1** and **2** in a PMMA Film[a)]

Substrate	Absorption band	Peak position /cm^{-1}	$f^2\Delta\bar{\alpha}$ /Å^{3} [b)]	$f\|\Delta\boldsymbol{\mu}\|$ /D[c)]
1	L_1	24220	50	2
	L_2	23530	12	—
	L_3	22970	26	—
	L_4	22590	−39	—
	Q band	17647	18 (16)	1 (1)
	Q band	16176	18 (16)	1 (1)
2	L_1	23620	35	2
	L_2	23000	57	—
	L_3	22515	7	—
	L_4	22150	−36	—
	Q band	17279	23 (44)	1 (1)
	Q band	15564	23 (44)	1 (1)

a) The values in parentheses were obtained from the electrophotoluminescence (E-PL) spectra. b) Experimental error 20%. c) Experimental error 30%; D = 3.34 × 10^{-30} C m.

The value of each of $\Delta\bar{\alpha}$ and $|\Delta\boldsymbol{\mu}|$ was evaluated for excitation at each absorption band from eqs 4 and 5. The results are shown in Table 1. Since it is difficult to determine the f value precisely, the $f^2\Delta\bar{\alpha}$ and $f|\Delta\boldsymbol{\mu}|$ values are evaluated using the unit of Å^3 and D (=3.34 × 10^{-30} C m), respectively. All of the first derivative spectra of the decomposed bands are used to fit the E-A spectra in Figures 3b and 3d, indicating that $\Delta\boldsymbol{\alpha}$ following photoexcitation is significant in the E-A spectra. The $f^2\Delta\bar{\alpha}$ value between the ground and excited states is estimated to be 50, 12, 26, and −39 Å^3 for L_1–L_4 of **1**, and 35, 57, 7, and −36 Å^3 for L_1–L_4 of **2**, respectively. These magnitudes of $\Delta\bar{\alpha}$ of **1** or **2** are smaller than the ones evaluated for the splitting Soret bands of *meso–meso*-linked porphyrin dimer,[18] which exhibits larger interaction between two porphyrins, and that the present values are roughly the same as the monomers of porphyrins such as tetraphenylporphyrin.[19,20] The magnitude of molecular polarizability reflects delocalization of electrons by an applied field in a molecular system. The present result suggests that the delocalization of electrons remains almost unchanged with the dimer formation of **1** and **2**. It may be different from the case of dimer appended with an electron acceptor, where photoinduced electron transfer produces a cation radical delocalized over two porphyrins.[22] It is also noted that, in the two strong bands of L_1 and L_3, the $\Delta\bar{\alpha}$ value of the L_1 band is larger than that of the L_3 band for both **1** and **2**. The L_4 band exhibits the negative $\Delta\bar{\alpha}$ value, indicating that the molecular polarizability decreases with excitation into the L_4 band, whereas the molecular polarizability increases with excitation into other absorption bands. The second derivative spectrum of the L_1 band is also necessary to reproduce the E-A spectra of **1** and **2**. The magnitude of $\Delta\boldsymbol{\mu}$ of the L_1 band is estimated to be

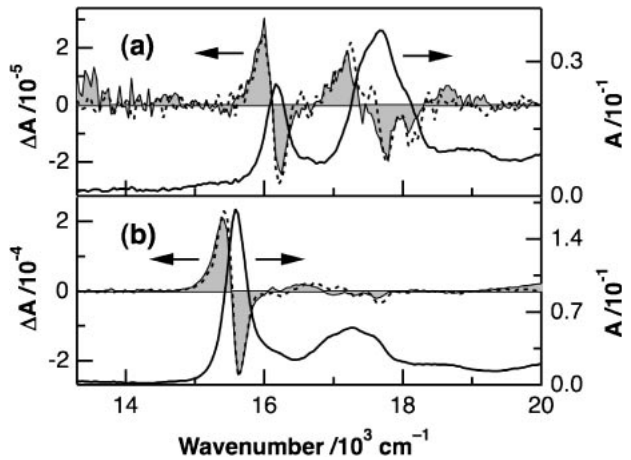

Figure 4. Electroabsorption spectra (shaded line) of **1** (a) and **2** (b) in a PMMA film in the Q band region together with the corresponding absorption spectra (solid line). The fitted spectra are also shown by a dotted line in each figure. Applied field strength was 0.7 MV cm^{-1}.

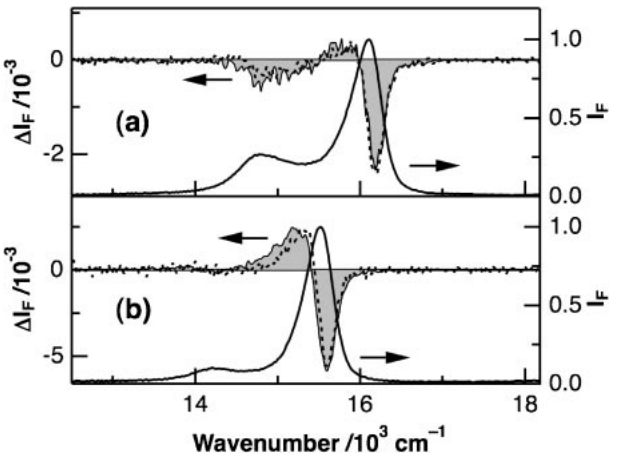

Figure 5. Photoluminescence spectra (solid line) and electrophotoluminescence spectra (shaded line) of **1** (a) and **2** (b) in a PMMA film. The fitted spectra are also shown by a dotted line in each figure. Applied field strength was 0.9 MV cm^{-1}.

ca. 2 D both for **1** and **2**. The zeroth derivative component was not necessary to fit the E-A spectra.

Figure 4 shows the E-A spectra of **1** and **2** in the Q band region. The E-A spectra in the Q band region are similar in shape to the first derivative of the corresponding absorption spectrum, although the small contribution of the second derivative spectrum is necessary to reproduce the E-A spectra. The $f^2\Delta\bar{\alpha}$ and $f|\Delta\boldsymbol{\mu}|$ values obtained for the Q bands are also shown in Table 1. Two bands are clearly observed in the Q band region however the band decomposition is not necessary to fit the E-A spectra in the Q band region (Figure 4), indicating that both bands give the same values of $\Delta\bar{\alpha}$ and $|\Delta\boldsymbol{\mu}|$. The minor components are also found to have similar $\Delta\bar{\alpha}$ and $|\Delta\boldsymbol{\mu}|$ values, resulting in the reproduction of the E-A spectra without band decomposition within the experimental accuracy. The different behavior between the Soret and Q bands is associated with different excited states of the two bands in general. Measurements of E-A spectra with a higher signal-to-noise ratio and analyses with theoretical calculations are needed to reach a more definitive conclusion on this point. The $\Delta\bar{\alpha}$ value of **2** obtained for the Q band region which is sensitive to the expansion of π-conjugation is larger than that of **1**, indicating the delocalization of π-electrons through the ethynyl group. It is noted that the splitting of the Q band due to the interaction between porphyrins is expected to be much smaller than that of the Soret band because the dipole–dipole interaction at the Q band is much smaller than that at the Soret band.

Figure 5 shows the E-PL spectra of **1** and **2** in a PMMA film, together with the PL spectra. Excitation wavelength was 414 and 434 nm for **1** and **2**, respectively, where the field-induced change in absorption intensity was negligible. The observed PL is assigned to the fluorescence emitted from **1** and **2**, i.e., fluorescence emitted from the excited states of the Q band. E-PL spectra shown in Figure 5 are similar in shape to the first derivative of the corresponding PL spectra, indicating that the field-induced change in fluorescence (PL) intensity mainly comes from $\Delta\boldsymbol{\alpha}$ following the fluorescence process. Actually, the E-PL spectra are reproduced by a linear combination among the zeroth, first, and second derivative spectra of the PL spectra. The values of $\Delta\bar{\alpha}$ and $|\Delta\boldsymbol{\mu}|$ obtained by the E-PL spectra of **1** and **2** are shown in Table 1. It was assumed in the evaluation that the molecular polarizability is isotropic, i.e., $\Delta\alpha_m = \Delta\bar{\alpha}$, and the angle-dependent term in eq 3 is negligible. The small difference in $\Delta\bar{\alpha}$ of the Q band between the E-A and E-PL spectra may be ascribed to the difference in electronic structure between the Franck–Condon (FC) excited state and the fluorescence excited state because the molecular structures of the FC state and the fluorescence state are different from each other. A small field-induced quenching of the fluorescence is also observed in both E-PL spectra, indicating that the non-radiative process from the fluorescence state of the porphyrin dimer is a little enhanced by ***F***. The magnitude of the field-induced decrease in the fluorescence yield is 0.06 and 0.05% for **1** and **2**, respectively, at 0.9 MV cm^{-1}. The band decomposition is not necessary to fit the E-PL spectra, although the two bands are clearly observed. This result is consistent with the E-A spectra in the Q band region mentioned above.

Conclusion

We have measured the E-A and E-PL spectra of two dimers of *meso*-imidazolyl-substituted zinc porphyrins in a PMMA polymer film. These dimers exhibit strong exciton coupling between the two porphyrins due to a slipped cofacial arrangement with a coordination of imidazolyl to zinc in non-polar solvents. The significant splitting of the Soret absorption band is observed in a PMMA polymer film, indicating that the slipped cofacial arrangement remains unchanged in a PMMA film. The E-A spectra in the Soret band region are well fitted by the deconvolution of the absorption spectrum into four components. The value of each of $\Delta\bar{\alpha}$ and $|\Delta\boldsymbol{\mu}|$ was evaluated for excitation at each absorption band. The measurements of field-induced changes in optical spectra are useful to identify bands that are hard to distinguish in a complicated optical spectrum.

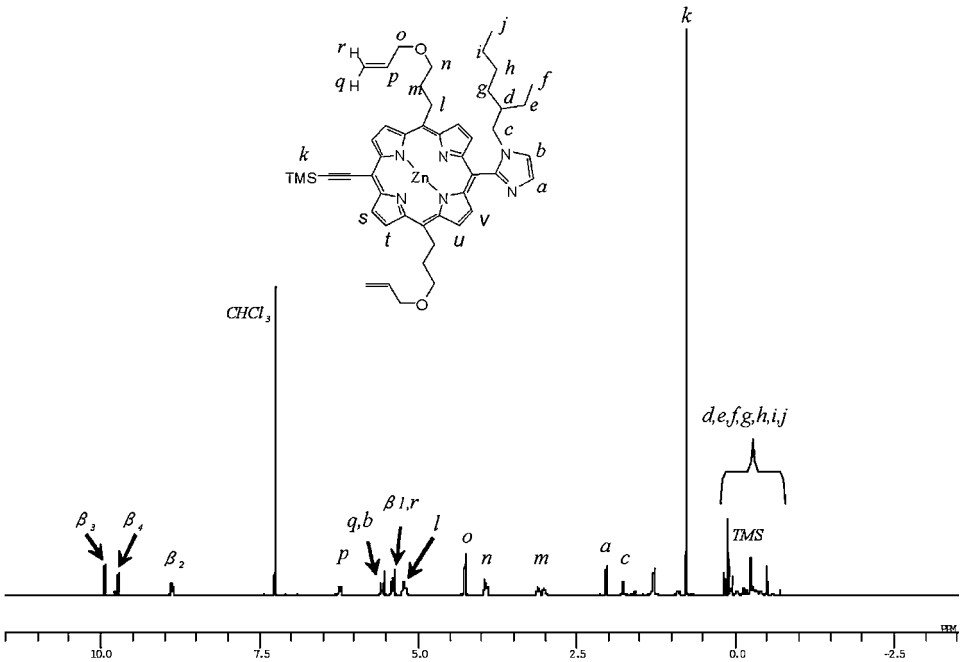

Figure 6. ^{1}H NMR spectrum of **2** in $CDCl_3$.

Experimental

PMMA (MW: 120000) was obtained from Aldrich and purified by precipitation with a mixture of benzene and methanol and by an extraction with hot methanol. A certain amount of benzene solution of PMMA containing porphyrin dimers was cast on an indium–tin–oxide (ITO)-coated quartz substrate by a spin coating, and the polymer film was dried to eliminate benzene. Then a semitransparent aluminum (Al) film was deposited on the dried polymer film by vacuum vapor deposition. The ITO and Al films were used as electrodes. The thickness of the film was typically 0.4 μm. E-A and E-PL spectra were measured using the same apparatus reported elsewhere.[17–19,21] A sinusoidal ac voltage with a modulation frequency of 40 Hz was applied between the ITO and Al films, and the value of the field-induced change in absorption intensity or PL intensity was detected with a lock-in amplifier at the second harmonic of the modulation frequency. A dc component of the transmitted light intensity or the PL intensity was simultaneously observed. The E-A and E-PL spectra were obtained by plotting the change in absorption intensity and in PL intensity as a function of wavelength, respectively. Applied field strength was estimated from the applied voltage divided by the polymer thickness. All the measurements were performed at room temperature. Compound **1** was synthesized according a procedure reported previously.[2]

5,15-Bis(3-allyloxypropyl)-20-[1-(2-ethylhexyl)imidazol-2-yl]-10-(trimethylsilylethynyl)porphyrin (3). 3-Trimethylsilyl-2-propynal (375 mg, 1.8 mmol), 1-(2-ethylhexyl)imidazol-2-carbaldehyde (227 mg, 1.8 mmol), and (3-allyloxypropyl)di-2-pyrrolylmethane (880 mg, 3.6 mmol) were dissolved in 720 mL of $CHCl_3$. The mixture was degassed by bubbling with N_2 for 10 min. Trifluoroacetic acid (TFA, 460 μL, 5.4 mmol) in $CHCl_3$ was added slowly to the stirred mixture. After stirring for 5 h, chloranil (1300 mg, 5.4 mol) was added. The mixture was then allowed to stir in the dark overnight at room temperature. The mixture was washed with saturated $NaHCO_3$ solution, brine and water and extracted with $CHCl_3$. The resulting crude product was chromatographed [Silica gel, 0–10% (v/v) MeOH in $CHCl_3$] for purification to afford pure material as a dark violet solid (93.6 mg, 6.7%). ^{1}H NMR (600 MHz, $CDCl_3$): δ 9.74 (d, $J = 4.8$ Hz, 2H, Por β), 9.52 (d, $J = 4.8$ Hz, 2H, Por β), 9.42 (d, $J = 4.8$ Hz, 2H, Por β), 8.73 (d, $J = 4.8$ Hz, 2H, Por β), 7.70 (d, $J = 1.1$ Hz, 1H, imidazole H_4), 7.48 (d, $J = 1.1$ Hz, 1H, imidazole H_5), 6.07 (m, 2H, CH_2=C*H*–), 5.43 (dd, $J = 17.4$, 1.2 Hz, 2H, C*H*$_2$=CH–), 5.28 (dd, $J = 10.8$, 1.2 Hz, 2H, C*H*$_2$=CH–), 5.04 (t, $J = 7.2$ Hz, 4H, Por–C*H*$_2$), 4.08 (dt, $J = 5.7$, 1.4 Hz, 4H, CH_2=CHC*H*$_2$–), 3.64 (t, $J = 5.7$ Hz, 4H, –OC*H*$_2$–), 3.59 (d, $J = 7.8$ Hz, 2H, –CH_2–), 2.83–2.70 (m, 4H, Por–CH_2C*H*$_2$–), 1.31–1.28 (m, 1H), 0.92–0.34 (m, 17H), 0.22–0.19 (m, 6H), −2.46 (s, 2H, inner NH). MS (MALDI-TOF Mass, dithranol); Found $m/z = 781.64$ [M + H$^+$], calcd for $C_{48}H_{60}N_6O_2Si$ 780.45.

5,15-Bis(3-allyloxypropyl)-20-[1-(2-ethylhexyl)imidazol-2-yl]-10-(trimethylsilylethynyl)porphyrinatozinc(II) (2). Into 20 mL of $CHCl_3$, **3** (54.9 mg, 70.3 μmol) was dissolved and 3 mL of a solution of zinc acetate dihydrate in MeOH (307 mg, 1.407 mmol) was added. After stirring for 30 min, the mixture was washed with brine and water and dried over anhydrous Na_2SO_4 (51.7 mg, 87%). This compound exists as dimer in $CHCl_3$. ^{1}H NMR (600 MHz, $CDCl_3$): δ 9.90 (d, 2H, $J = 4.2$ Hz, Por β), 9.69 (m, 2H, Por β), 8.85 (m, 2H, Por β), 6.20–6.19 (m, 2H, CH_2=C*H*–), 5.53 (d, 2H, $J = 17.4$ Hz, C*H*$_2$=CH–), 5.49 (s, 1H, imidazole), 5.39–5.35 (m, 4H, C*H*$_2$=CH–, Por β), 5.21–5.18 (m, 4H, Por–C*H*$_2$), 4.28–4.23 (m, 4H, CH_2=CHC*H*$_2$–), 3.94–3.91 (m, 4H, CH_2=CHC*H*$_2$–), 3.08–2.97 (m, 4H, –CH_2–), 2.01 (s, 1H, imidazole), 1.74 (s, 2H, CH_2), 0.74 (s, 9H, TMS), 0.04–−0.53 (m, 15H, ethylhexyl). The ^{1}H NMR spectrum of **2** is shown in Figure 6. MS (MALDI-TOF Mass, dithranol); Found $m/z = 843.51$ [M + H$^+$], calculated for $C_{48}H_{58}N_6O_2SiZn$ 842.368.

This work was supported by Grants-in-Aid for Scientific Research (Grant Nos. 20245001 and 18750118) from the Ministry of Education, Culture, Sports, Science and Technology (MEXT) in Japan.

References

1 Y. Kobuke, H. Miyaji, *J. Am. Chem. Soc.* **1994**, *116*, 4111.
2 A. Ohashi, A. Satake, Y. Kobuke, *Bull. Chem. Soc. Jpn.* **2004**, *77*, 365.
3 K. Ogawa, Y. Kobuke, *J. Photochem. Photobiol., C* **2006**, *7*, 1.
4 H. Imahori, *J. Phys. Chem. B* **2004**, *108*, 6130.
5 M. R. Wasielewski, *Chem. Rev.* **1992**, *92*, 435.
6 A. K. Burrell, D. L. Officer, P. G. Plieger, D. C. W. Reid, *Chem. Rev.* **2001**, *101*, 2751.
7 Y. Nakamura, N. Aratani, A. Osuka, *Chem. Soc. Rev.* **2007**, *36*, 831.
8 S. Fukuzumi, *Phys. Chem. Chem. Phys.* **2008**, *10*, 2283.
9 K. Ogawa, Y. Kobuke, *Angew. Chem., Int. Ed.* **2000**, *39*, 4070.
10 K. Ogawa, T. Zhang, K. Yoshihara, Y. Kobuke, *J. Am. Chem. Soc.* **2002**, *124*, 22.
11 K. Ogawa, A. Ohashi, Y. Kobuke, K. Kamada, K. Ohta, *J. Am. Chem. Soc.* **2003**, *125*, 13356.
12 W. Liptay, in *Excited States*, ed. by E. C. Lim, Academic Press, New York, **1974**, Vol. 1, p. 129.
13 G. U. Bublitz, S. G. Boxer, *Annu. Rev. Phys. Chem.* **1997**, *48*, 213.
14 N. Ohta, *Bull. Chem. Soc. Jpn.* **2002**, *75*, 1637.
15 S. G. Boxer, *J. Phys. Chem. B* **2009**, *113*, 2972.
16 E. Jalviste, N. Ohta, *J. Photochem. Photobiol., C* **2007**, *8*, 30.
17 T. Nakabayashi, Md. Wahadoszamen, N. Ohta, *J. Am. Chem. Soc.* **2005**, *127*, 7041.
18 N. Ohta, Y. Iwaki, T. Ito, I. Yamazaki, A. Osuka, *J. Phys. Chem. B* **1999**, *103*, 11242.
19 Y. Iwaki, N. Ohta, *Chem. Lett.* **2000**, 894.
20 W. Stampor, *Chem. Phys.* **2004**, *305*, 77.
21 S. Umeuchi, Y. Nishimura, I. Yamazaki, H. Murakami, M. Yamashita, N. Ohta, *Thin Solid Films* **1997**, *311*, 239.
22 H. Ozeki, A. Nomoto, K. Ogawa, Y. Kobuke, M. Murakami, K. Hosoda, M. Ohtani, S. Nakashima, H. Miyasaka, T. Okada, *Chem.—Eur. J.* **2004**, *10*, 6393.